

---

# Balanced Meta-Softmax for Long-Tailed Visual Recognition

---

Jiawei Ren<sup>1</sup>, Cunjun Yu<sup>1</sup>, Shunan Sheng<sup>1,2</sup>, Xiao Ma<sup>1,3</sup>, Haiyu Zhao<sup>1\*</sup>, Shuai Yi<sup>1</sup>, Hongsheng Li<sup>4</sup>

<sup>1</sup> SenseTime Research

<sup>2</sup> Nanyang Technological University

<sup>3</sup> National University of Singapore

<sup>4</sup> The Chinese University of Hong Kong

{renjiawei, yucunjun, zhaohaiyu, yishuai}@sensetime.com

shen0152@e.ntu.edu.sg xiao-ma@comp.nus.edu.sg hsli@ee.cuhk.edu.hk

## Abstract

Deep classifiers have achieved great success in visual recognition. However, real-world data is long-tailed by nature, leading to the mismatch between training and testing distributions. In this paper, we show that Softmax function, though used in most classification tasks, gives a biased gradient estimation under the long-tailed setup. This paper presents Balanced Softmax, an elegant unbiased extension of Softmax, to accommodate the label distribution shift between training and testing. Theoretically, we derive the generalization bound for multiclass Softmax regression and show our loss minimizes the bound. In addition, we introduce Balanced Meta-Softmax, applying a complementary Meta Sampler to estimate the optimal class sample rate and further improve long-tailed learning. In our experiments, we demonstrate that Balanced Meta-Softmax outperforms state-of-the-art long-tailed classification solutions on both visual recognition and instance segmentation tasks.

## 1 Introduction

Most real-world data comes with a long-tailed nature: a few high-frequency classes (or head classes) contributes to most of the observations, while a large number of low-frequency classes (or tail classes) are under-represented in data. Taking an instance segmentation dataset, LVIS [9], for example, the number of instances in *banana* class can be thousands of times more than that of a *bait* class. In practice, the number of samples per class generally decreases from head to tail classes exponentially. Under the power law, the tails can be undesirably heavy. A model that minimizes empirical risk on long-tailed training datasets often underperforms on a class-balanced test dataset. As datasets are scaling up nowadays, the long-tailed nature poses critical difficulties to many vision tasks, e.g., visual recognition and instance segmentation.

An intuitive solution to long-tailed task is to re-balance the data distribution. Most state-of-the-art (SOTA) methods use the class-balanced sampling or loss re-weighting to “simulate” a balanced training set [3, 35]. However, they may under-represent the head class or have gradient issues during optimization. Cao et al. [4] introduced Label-Distribution-Aware Margin Loss (LDAM), from the perspective of the generalization error bound. Given fewer training samples, a tail class should have a higher generalization error bound during optimization. Nevertheless, LDAM is derived from the hinge loss, under a binary classification setup and is not suitable for multi-label classification.

We propose *Balanced Meta-Softmax* (BALMS) for long-tailed visual recognition. We first show that the Softmax function is intrinsically biased under the long-tailed scenario. We derive a Balanced

---

\*Corresponding author

Softmax function from the probabilistic perspective that explicitly models the test-time label distribution shift. Theoretically, we found that optimizing for the Balanced Softmax cross-entropy loss is equivalent to minimizing the generalization error bound. Balanced Softmax generally improves long-tailed classification performance on datasets with moderate imbalance ratios, e.g., CIFAR-10-LT [21] with a maximum imbalance factor of 200. However, for datasets with an extremely large imbalance factor, e.g., LVIS [9] with an imbalance factor of 26,148, the optimization process becomes difficult. Complementary to the loss function, we introduce the *Meta Sampler*, which learns to re-sample for achieving high validation accuracy by meta-learning. The combination of Balanced Softmax and Meta Sampler could efficiently address long-tailed classification tasks with high imbalance factors.

We evaluate BALMS on both long-tailed image classification and instance segmentation on five commonly used datasets: CIFAR-10-LT [21], CIFAR-100-LT [21], ImageNet-LT [26], Places-LT [37] and LVIS [9]. On all datasets, BALMS outperforms state-of-the-art methods. In particular, BALMS outperforms all SOTA methods on LVIS, with an extremely high imbalanced factor, by a large margin.

We summarize our contributions as follows: 1) we theoretically analyze the incapability of Softmax function in long-tailed tasks; 2) we introduce Balanced Softmax function that explicitly considers the generalization error bound during optimization; 3) we present the Meta Sampler, a meta-learning based re-sampling strategy for long-tailed learning.

## 2 Related Works

**Data Re-Balancing.** Pioneer works focus on re-balancing during training. Specifically, re-sampling strategies [3, 22, 5, 10, 12, 31, 2, 1] try to restore the true distributions from the imbalanced training data. Re-weighting, i.e., cost-sensitive learning[35, 13, 14, 19, 28], assigns a cost weight to the loss of each class. However, it is argued that over-sampling inherently overfits the tail classes and under-sampling under-represents head classes’ rich variations. Meanwhile, re-weighting tends to cause unstable training especially when the class imbalance is severe because there would be abnormally large gradients when the weights are very large.

**Loss Function Engineering.** Tan et al. [34] pointed out that randomly dropping some scores of tail classes in the Softmax function can effectively help, by balancing the positive gradients and negative gradients flowing through the score outputs. Cao et al. [4] showed that the generalization error bound could be minimized by increasing the margins of tail classes. Khan et al. [11] modify the loss function based on Bayesian uncertainty. Li et al. [23] proposes two novel loss functions to balance the gradient flow. Nevertheless, as we show in this paper, Softmax function, which is commonly adopted in these methods, is biased under the long-tailed scenarios. Our proposed method with Balanced Softmax addresses the issue and significantly improves the standard loss-based methods.

**Meta-Learning.** Many approaches [15, 30, 32] have been proposed to tackle the long-tailed issue with meta-learning. Many of them focused on optimizing the weight-per-sample as a learnable parameter, which appears as a hyper-parameter in the re-weight approach. This group of methods requires a clean and unbiased dataset as a meta set, i.e., development set, which is usually a fixed subset of the training images and use bi-level optimization to estimate the weight parameter.

**Decoupled Training.** A few recent works [18, 38] point out that decoupled training, a simple yet effective solution, could significantly improve the generalization issue on long-tailed datasets. The classifier is the only under-performed component when training in imbalanced datasets. However, in our experiments, we found this technique is not adequate for datasets with extremely high imbalance factors, e.g., LVIS [9]. Interestingly in our experiments, we observed that decoupled training is complementary to our proposed BALMS, and combining them results in additional improvements.

## 3 Balanced Meta-Softmax

The major challenge for long-tailed visual recognition is the mismatch between training data distribution and test data distribution. Let  $\mathcal{X} = \{x_i, y_i\}, i \in \{1, \dots, n\}$  be the balanced testing set, where  $x_i$  denotes a data point and  $y_i$  denotes its label. Let  $k$  be the number of classes,  $n_j$  be the number of samples in class  $j$ , where  $\sum_{j=1}^k n_j = n$ . Similarly, we denote the long-tailed training set as  $\hat{\mathcal{X}} = \{\hat{x}_i, \hat{y}_i\}, i \in \{1, \dots, n\}$ . Normally, we have  $\forall i, p(\hat{y}_i) \neq p(y_i)$ . Specifically, for a tail class  $j$ ,  $p(\hat{y}_j) \ll p(y_j)$ , which makes the generalization under long-tailed scenarios extremely challenging.

We introduce Balanced Meta-Softmax (BALMS) for long-tailed visual recognition. It has two components: 1) a Balanced Softmax function that accommodates the label distribution shift between training and testing; 2) a Meta Sampler that learns to re-sample training set by meta-learning. We denote a feature extractor function as  $f$  and a linear classifier's weight as  $\theta$ .

### 3.1 Balanced Softmax

**Label Distribution Shift.** We begin by revisiting the multi-class Softmax regression, where we are generally interested in estimating the conditional probability  $p(y|x)$ , which can be modeled as a multinomial distribution  $\phi$ :

$$\phi = \phi_1^{\mathbf{1}\{y=1\}} \phi_2^{\mathbf{1}\{y=2\}} \dots \phi_k^{\mathbf{1}\{y=k\}}; \quad \phi_j = \frac{e^{\eta_j}}{\sum_{i=1}^k e^{\eta_i}}; \quad \sum_{j=1}^k \phi_j = 1 \quad (1)$$

where  $\mathbf{1}(\cdot)$  is the indicator function and Softmax function maps a model's class- $j$  output  $\eta_j = \theta_j^T f(x)$  to the conditional probability  $\phi_j$ .

From the Bayesian inference's perspective,  $\phi_j$  can also be interpreted as:

$$\phi_j = p(y = j|x) = \frac{p(x|y = j)p(y = j)}{p(x)} \quad (2)$$

where  $p(y = j)$  is in particular interest under the class-imbalanced setting. Assuming that all instances in the training dataset and the test dataset are generated from the same process  $p(x|y = j)$ , there could still be a discrepancy between training and testing given different label distribution  $p(y = j)$  and evidence  $p(x)$ . With a slight abuse of the notation, we re-define  $\phi$  to be the conditional distribution on the balanced test set and define  $\hat{\phi}$  to be the conditional probability on the imbalanced training set. As a result, standard Softmax provides a biased estimation for  $\phi$ .

**Balanced Softmax.** To eliminate the discrepancy between the posterior distributions of training and testing, we introduce the Balanced Softmax. We use the same model outputs  $\eta$  to parameterize two conditional probabilities:  $\phi$  for testing and  $\hat{\phi}$  for training.

**Theorem 1.** Assume  $\phi$  to be the desired conditional probability of the balanced data set, with the form  $\phi_j = p(y = j|x) = \frac{p(x|y=j)}{p(x)} \frac{1}{k}$ , and  $\hat{\phi}$  to be the desired conditional probability of the imbalanced training set, with the form  $\hat{\phi}_j = \hat{p}(y = j|x) = \frac{p(x|y=j)}{\hat{p}(x)} \frac{n_j}{\sum_{i=1}^k n_i}$ . If  $\phi$  is expressed by the standard Softmax function of model output  $\eta$ , then  $\hat{\phi}$  can be expressed as

$$\hat{\phi}_j = \frac{n_j e^{\eta_j}}{\sum_{i=1}^k n_i e^{\eta_i}}. \quad (3)$$

We use the exponential family parameterization to prove Theorem 1. The proof can be found in the supplementary materials. Theorem 1 essentially shows that applying the following Balanced Softmax function can naturally accommodate the label distribution shifts between the training and test sets. We define the Balanced Softmax function as

$$\hat{l}(\theta) = -\log(\hat{\phi}_y) = -\log\left(\frac{n_y e^{\eta_y}}{\sum_{i=1}^k n_i e^{\eta_i}}\right). \quad (4)$$

We further investigate the improvement brought by the Balanced Softmax in the following sections.

Many vision tasks, e.g., instance segmentation, might use multiple binary logistic regressions instead of a multi-class Softmax regression. By virtue of Bayesian law, a similar strategy can be applied to the multiple binary logistic regressions. The detailed derivation is left in the supplementary materials.

#### Generalization Error Bound

Generalization error bound gives the upper bound of a model's test error, given its training error. With dramatically fewer training samples, the tail classes have much higher generalization bounds than the head classes, which make high classification accuracy on tail classes unlikely. In this section, we show that optimizing Eqn. 4 is equivalent to minimizing the generalization upper bound.

Margin theory provides a bound based on the margins [17]. Margin bounds usually negatively correlate to the magnitude of the margin, i.e., larger margin leads to lower generalization error. Consequently, given a constraint on the sum of margins of all classes, there would be a trade-off between minority classes and majority classes [4].

Locating such an optimal margin for multi-class classification is non-trivial. The bound investigated in [4] was established for binary classification using hinge loss. Here, we try to develop the margin bound for the multi-class Softmax regression. Given the previously defined  $\phi$  and  $\hat{\phi}$ , we derive  $\hat{l}(\theta)$  by minimizing the margin bound. Margin bound commonly bounds the 0-1 error:

$$err_{0,1} = \Pr \left[ \theta_y^T f(x) < \max_{i \neq y} \theta_i^T f(x) \right]. \quad (5)$$

However, directly using the 0-1 error as the loss function is not ideal for optimization. Instead, negative log likelihood (NLL) is generally considered more suitable. With continuous relaxation of Eqn. 5, we have

$$err(t) = \Pr[t < \log(1 + \sum_{i \neq y} e^{\theta_i^T f(x) - \theta_y^T f(x)})] = \Pr[l(\theta) > t], \quad (6)$$

where  $t \geq 0$  is any threshold, and  $l_y(\theta)$  is a standard negative log-likelihood with Softmax. This new error is still a counter, but describes how likely the test loss will be larger than a given threshold. Naturally, we define our margin for class  $j$  to be

$$\gamma_j = t - \max_{(x,y) \in S_j} l_j(\theta). \quad (7)$$

where  $S_j$  is the set of all class  $j$  samples. If we force a large margin  $\gamma_j$  during training, i.e., force the training loss to be much lower than  $t$ , then  $err(t)$  will be reduced. The Theorem 2 in [17] can then be directly generalized as

**Theorem 2.** *Let  $t \geq 0$  be any threshold, for all  $\gamma_j > 0$ , with probability at least  $1 - \delta$ , we have*

$$err_{bal}(t) \lesssim \frac{1}{k} \sum_{j=1}^k \left( \frac{1}{\gamma_j} \sqrt{\frac{C}{n_j}} + \frac{\log n}{\sqrt{n_j}} \right); \quad \gamma_j^* = \frac{\beta n_j^{-1/4}}{\sum_{i=1}^k n_i^{-1/4}}, \quad (8)$$

where  $err_{bal}(t)$  is the error on the balanced test set,  $\lesssim$  is used to hide constant terms and  $C$  is some measure on complexity. With a constraint on  $\sum_{j=1}^k \gamma_j = \beta$ , Cauchy-Schwarz inequality gives us the optimal  $\gamma_j^*$ .

The optimal  $\gamma^*$  suggests that we need larger  $\gamma$  for the classes with fewer samples. In other words, to achieve the optimal generalization ability, we need to focus on minimizing the training loss of the tail classes. Therefore, for each class  $j$ , the desired training loss  $\hat{l}_j^*(\theta)$  is

$$\hat{l}_j^*(\theta) = l_j(\theta) + \gamma_j^*, \quad \text{where } l_j(\theta) = -\log(\phi_j), \quad (9)$$

**Corollary 2.1.**  $\hat{l}_j^*(\theta) = l_j(\theta) + \gamma_j^* = l_j(\theta) + \frac{\beta n_j^{-1/4}}{\sum_{i=1}^k n_i^{-1/4}}$  can be approximated by  $\hat{l}_j(\theta)$  when:

$$\hat{l}_j(\theta) = -\log(\hat{\phi}_j); \quad \hat{\phi}_j = \frac{e^{\eta_j - \log \gamma_j^*}}{\sum_{i=1}^k e^{\eta_i - \log \gamma_i^*}} = \frac{n_j^{\frac{1}{4}} e^{\eta_j}}{\sum_{i=1}^k n_i^{\frac{1}{4}} e^{\eta_i}} \quad (10)$$

We provide a sketch of proof to the corollary in supplementary materials. Notice that compared to Eqn. 4, we have an additional constant  $1/4$  before  $\log n_j$ . We empirically find that setting  $1/4$  to 1 leads to the optimal results, which may suggest that Eqn. 41 is not necessarily tight. To this point, the label distribution shift and generalization bound of multi-class Softmax regression lead us to the same loss form: Eqn. 4.

### 3.2 Meta Sampler

Although the Balanced Softmax theoretically optimizes the generalization error bound, given larger datasets with extremely imbalanced data distribution, the optimization is still challenging.

Class-balanced sampler (CBS) is used to tweak the mini-batches' sampling process and fine-tune the classifier in the decoupled training setup [18, 38]. It potentially helps to simplify the optimization landscape by choosing class-balanced samples. However, in our experiments, we found that naively combining CBS with Balanced Softmax worsens the performance.

We first theoretically analyze the cause of the performance drop. When the linear classifier's weight  $\theta_j$  for class  $j$  has converged, i.e.,  $\sum_{s=1}^B \frac{\partial L^{(s)}}{\partial \theta_j} = 0$ , we have:

$$\sum_{s=1}^B \frac{\partial L^{(s)}}{\partial \theta_j} = \sum_{s=1}^{B/k} f(x_{y=j}^{(s)})(1 - \hat{\phi}_j^{(s)}) - \sum_{i \neq j} \sum_{s=1}^{B/k} f(x_{y=i}^{(s)})\hat{\phi}_j^{(s)} = 0, \quad (11)$$

where  $B$  is the batch size and  $k$  is the number of classes. Samples per class have been ensured to be  $B/k$  by CBS. When the classification loss converges to 0, the conditional probability of the correct class  $\hat{\phi}_j$  is expected to be close to 1. For any positive sample  $x^+$  and negative sample  $x^-$  of class  $j$ , we have  $\hat{\phi}_j(x^+) \approx \phi_j(x^+)$  and  $\hat{\phi}_j(x^-) \approx \frac{n_j}{n_i} \phi_j(x^-)$ , when  $\hat{\phi}_j \rightarrow 1$ . Eqn. 11 can be rewritten as

$$\frac{1}{n_j^2} \mathbb{E}_{(x^+, y=j) \sim D_{train}} [f(x^+)(1 - \phi_j)] - \sum_{i \neq j} \frac{1}{n_i^2} \mathbb{E}_{(x^-, y=i) \sim D_{train}} [f(x^-)\phi_j] \approx 0 \quad (12)$$

where  $D_{train}$  is the training set. The formal derivation of Eqn. 12 is in the supplementary materials.

Compared to the inverse loss weight, i.e.,  $1/n_j$  for class  $j$ , combining Balanced Softmax with CBS leads to the over-balance problem, i.e.,  $1/n_j^2$  for class  $j$ , which deviates from the optimal distribution.

### Meta Sampler

To simplify the gradient descent process with CBS, we introduce a learnable version of it based on meta-learning, which is named Meta Sampler. We first define the empirical loss by sampling from dataset  $D$  as  $L_D(\theta) = \mathbb{E}_{(x,y) \sim D} [l(\theta)]$  for standard Softmax, and  $\hat{L}_D(\theta) = \mathbb{E}_{(x,y) \sim D} [\hat{l}(\theta)]$  for Balanced Softmax, where  $\hat{l}(\theta)$  is defined previously in Eqn. 4.

To estimate the optimal sample rates for different classes, we adopt a bi-level meta-learning strategy: we update the parameter  $\psi$  of sample distribution  $\pi_\psi$  in the inner loop and update the classifier parameters  $\theta$  in the outer loop,

$$\pi_\psi^* = \arg \min_{\psi} L_{D_{meta}}(\theta^*(\pi_\psi)) \quad s.t. \quad \theta^*(\pi_\psi) = \arg \min_{\theta} \hat{L}_{D_{q(x,y;\pi_\psi)}}(\theta), \quad (13)$$

where  $\pi_\psi^j = p(y = j; \psi)$  is the sample rate for class  $j$ ,  $D_{q(x,y;\pi_\psi)}$  is the training set with class sample distribution  $\pi_\psi$ , and  $D_{meta}$  is a meta set we introduce to supervise the outer loop optimization. We create the meta set by class-balanced sampling from the training set  $D_{train}$ . Empirically, we found it sufficient for inner loop optimization. An intuition to this bi-level optimization strategy is that: we want to learn best sample distribution parameter  $\psi$  such that the network, parameterized by  $\theta$ , outputs best performance on meta dataset  $D_{meta}$  when trained by samples from  $\pi_\psi$ .

We first compute the per-instance sample rate  $\rho_i = \pi_\psi^{c(i)} / \sum_{i=1}^n \pi_\psi^{c(i)}$ , where  $c(i)$  denotes the label class for instance  $i$  and  $n$  is total number of training samples, and sample a training batch  $B_\psi$  from a parameterized multi-nomial distribution  $\rho$ . Then we optimize the model in a meta-learning setup by

1. sample a mini-batch  $B_\psi$  given distribution  $\pi_\psi$  and perform one step gradient descent to get a surrogate model parameterized by  $\tilde{\theta}$  by  $\tilde{\theta} \leftarrow \theta - \nabla_{\theta} \tilde{L}_{B_\psi}(\theta)$ .
2. compute the  $L_{D_{meta}}(\tilde{\theta})$  of the surrogate model on the meta dataset  $D_{meta}$  and optimize the sample distribution parameter by  $\psi \leftarrow \psi - \nabla_{\psi} L_{D_{meta}}(\tilde{\theta})$  with cross-entropy loss with standard Softmax
3. update the model parameter  $\theta \leftarrow \theta - \nabla_{\theta} \hat{L}_{B_\psi}(\theta)$  with Balanced Softmax

However, sampling from a discrete distribution is not differentiable by nature. To allow end-to-end training for the sampling process, when forming the mini-batch  $B_\psi$ , we apply the Gumbel-Softmax reparameterization trick [16]. A detailed explanation can be found in the supplementary materials.

If we apply Meta Sampler with standard cross-entropy loss with Softmax, the convergence would be relatively slow when the class-imbalance factor is high. In addition, it might overfit the tail class and underfit the head class. In BALMS, the Balanced Softmax alleviates this issue because it naturally balances the distribution, as shown in Eqn. 12. Thus, the Meta Sampler could output a relatively more balanced sample distribution. We provide additional discussions in the experiments.

## 4 Experiments

### 4.1 Experimental Setup

**Datasets.** We perform experiments on long-tailed image classification datasets, including CIFAR-10-LT [21], CIFAR-100-LT [21], ImageNet-LT [26] and Places-LT [37] and one long-tailed instance segmentation dataset, LVIS [9]. We define the imbalance factor of a dataset as the number of training instances in the largest class divided by that of the smallest. Details of datasets are in Table 1.

**Evaluation Setup.** For classification tasks, after training on the long-tailed dataset, we evaluate the models on the corresponding balanced test/validation dataset and report top-1 accuracy. We also report accuracy on three splits of the set of classes: Many-shot (more than 100 images), Medium-shot (20  $\sim$  100 images), and Few-shot (less than 20 images). Notice that results on small datasets, i.e., CIFAR-LT 10/100, tend to show large variances, we report the mean and standard error under 3 repetitive experiments. We show details of long-tailed dataset generation in supplementary materials. For LVIS, we use official training and testing splits. Average Precision (AP) in COCO style [24] for both bounding box and instance mask are reported. Our implementation details can be found in the supplementary materials.

Dataset	#Classes	Imbalance Factor
CIFAR-10-LT [21]	10	10-200
CIFAR-100-LT [21]	100	10-200
ImageNet-LT [26]	1,000	256
Places-LT [37]	365	996
LVIS [9]	1,230	26,148

Table 1: Details of long-tailed datasets. For both CIFAR-10 and CIFAR-100, we report results with different imbalance factors.

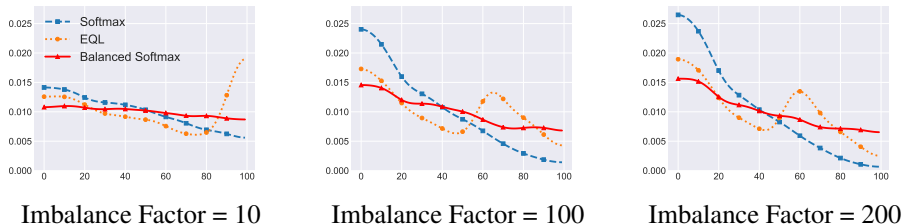


Figure 1: Experiment on CIFAR-100-LT. x-axis is the class labels with decreasing training samples and y-axis is the marginal likelihood  $p(y)$ . Balanced Softmax is more stable under a high imbalance factor compared to the Softmax baseline and SOTA method, Equalization Loss(EQL).

### 4.2 Long-Tailed Image Classification

We present the results for long-tailed image classification in Table 2 and Table 3. On all datasets, BALMS achieves SOTA performance compared with all end-to-end training and decoupled training methods. In particular, we notice that BALMS demonstrates a clear advantage under two cases: 1) When the imbalance factor is high. For example, on CIFAR-10 with an imbalance factor of 200, BALMS is higher than the SOTA method, LWS [18], by 3.4%. 2) When the dataset is large. BALMS achieves comparable performance with cRT on ImageNet-LT, which is a relatively small dataset, but it significantly outperforms cRT on a larger dataset, Places-LT.

In addition, we study the robustness of the proposed Balanced Softmax compared to standard Softmax and SOTA loss function for long-tailed problems, EQL [34]. We visualize the marginal likelihood  $p(y)$  trained with a different loss given different imbalance factors in Fig. 1. Balanced Softmax clearly gives a smoother and more balanced likelihood under different imbalance factors.

Dataset	CIFAR-10-LT			CIFAR-100-LT		
Imbalance Factor	200	100	10	200	100	10
End-to-end training						
Softmax	71.2 $\pm$ 0.3	77.4 $\pm$ 0.8	90.0 $\pm$ 0.2	41.0 $\pm$ 0.3	45.3 $\pm$ 0.3	61.9 $\pm$ 0.1
CBW	72.5 $\pm$ 0.2	78.6 $\pm$ 0.6	90.1 $\pm$ 0.2	36.7 $\pm$ 0.2	42.3 $\pm$ 0.8	61.4 $\pm$ 0.3
CBS	68.3 $\pm$ 0.3	77.8 $\pm$ 2.2	90.2 $\pm$ 0.2	37.8 $\pm$ 0.1	42.6 $\pm$ 0.4	61.2 $\pm$ 0.3
Focal Loss [25]	71.8 $\pm$ 2.1	77.1 $\pm$ 0.2	90.3 $\pm$ 0.2	40.2 $\pm$ 0.5	43.8 $\pm$ 0.1	60.0 $\pm$ 0.6
Class Balance Loss [6]	72.6 $\pm$ 1.8	78.2 $\pm$ 1.1	89.9 $\pm$ 0.3	39.9 $\pm$ 0.1	44.6 $\pm$ 0.4	59.8 $\pm$ 1.1
LDAM [4]	71.2 $\pm$ 0.3	77.2 $\pm$ 0.2	90.2 $\pm$ 0.3	41.0 $\pm$ 0.3	45.4 $\pm$ 0.1	62.0 $\pm$ 0.3
Equalization Loss [34]	72.8 $\pm$ 0.2	76.7 $\pm$ 0.1	89.9 $\pm$ 0.3	43.3 $\pm$ 0.1	47.3 $\pm$ 0.1	59.7 $\pm$ 0.3
Decoupled training						
cRT [18]	76.6 $\pm$ 0.2	82.0 $\pm$ 0.2	91.0 $\pm$ 0.0	44.5 $\pm$ 0.1	50.0 $\pm$ 0.2	63.3 $\pm$ 0.1
LWS [18]	78.1 $\pm$ 0.0	83.7 $\pm$ 0.0	91.1 $\pm$ 0.0	45.3 $\pm$ 0.1	50.5 $\pm$ 0.1	<b>63.4</b> $\pm$ 0.1
BALMS	<b>81.5</b> $\pm$ 0.0	<b>84.9</b> $\pm$ 0.1	<b>91.3</b> $\pm$ 0.1	<b>45.5</b> $\pm$ 0.1	<b>50.8</b> $\pm$ 0.0	63.0 $\pm$ 0.1

Table 2: Top 1 accuracy for CIFAR-10/100-LT. Softmax denotes the standard cross-entropy loss with Softmax, CBW denotes class-balanced weighting and CBS denotes class-balanced sampling. BALMS generally outperforms SOTA methods, especially when the imbalance factor is high. Note that for other methods, we reproduce higher accuracy than reported in original papers.

Dataset	ImageNet-LT				Places-LT			
Accuracy	Many	Medium	Few	Overall	Many	Medium	Few	Overall
End-to-end training								
Lifted Loss [33]	35.8	30.4	17.9	30.8	41.1	35.4	24	35.2
Focal Loss [25]	36.4	29.9	16	30.5	41.1	34.8	22.4	34.6
Range Loss [36]	35.8	30.3	17.6	30.7	41.1	35.4	23.2	35.1
OLTR [26]	43.2	35.1	18.5	35.6	<b>44.7</b>	37.0	25.3	35.9
Equalization Loss [34]	-	-	-	36.4	-	-	-	-
Decoupled training								
cRT [18]	-	-	-	<b>41.8</b>	42.0	37.6	24.9	36.7
LWS [18]	-	-	-	41.4	40.6	39.1	28.6	37.6
BALMS	<b>50.3</b>	<b>39.5</b>	<b>25.3</b>	<b>41.8</b>	41.2	<b>39.8</b>	<b>31.6</b>	<b>38.7</b>

Table 3: Top 1 Accuracy on ImageNet-LT and Places-LT. We present results with ResNet-10 [26] for ImageNet-LT and ImageNet pre-trained ResNet-152 for Places-LT. Baseline results are taken from original papers. BALMS generally outperforms the SOTA models.

### 4.3 Long-Tailed Instance Segmentation

LVIS dataset is one of the most challenging datasets in the vision community. As suggested in Tabel 1, the dataset has a much higher imbalance factor compared to the rest (26148 vs. less than 1000) and contains many very few-shot classes. Compared to the image classification datasets, which are relatively small and have lower imbalance factors, the LVIS dataset gives a more reliable evaluation of the performance of long-tailed learning methods.

Since one image might contain multiple instances from several categories, we hereby use Meta Reweigher instead of Meta Sampler. As shown in Table 4, BALMS achieves the best results among all the approaches and outperform others by a large margin, especially on rare classes, where BALMS achieves an average precision of 19.6 while the best of the rest is 14.6. The results suggest that with the Balanced Softmax function and learnable Meta Reweigher, BALMS is able to give more balanced gradients and tackles the extremely imbalanced long-tailed tasks.

In particular, LVIS is composed of images of complex daily scenes with natural long-tailed categories. To this end, we believe BALMS is applicable to real-world long-tailed visual recognition challenges.

### 4.4 Component Analysis

We conduct an extensive component analysis on CIFAR-10/100-LT dataset to further understand the effect of each proposed component of BALMS. The results are presented in Table 5.

Method	$AP_m$	$AP_f$	$AP_c$	$AP_r$	$AP_b$
Softmax	23.7	27.3	24.0	13.6	24.0
Sigmoid	23.6	27.3	24.0	12.7	24.0
Focal Loss [25]	23.4	<b>27.5</b>	23.5	12.8	23.8
Class Balance Loss [6]	23.3	27.3	23.8	11.4	23.9
LDAM [4]	24.1	26.3	25.3	14.6	24.5
LWS [18]	23.8	26.8	24.4	14.4	24.1
Equalization Loss [34]	25.2	26.6	27.3	14.6	25.7
BALMS	<b>27.0</b>	<b>27.5</b>	<b>28.9</b>	<b>19.6</b>	<b>27.6</b>

Table 4: Results for LVIS dataset.  $AP_m$  denotes Average Precision of masks.  $AP_b$  denotes Average Precision of bounding box.  $AP_f$ ,  $AP_c$  and  $AP_r$  denote Average Precision of masks on frequent classes, common classes and rare classes. BALMS significantly outperforms SOTA models given high imbalance factor in LVIS. Other methods are reproduced with higher AP than reported if given.

Dataset	CIFAR-10-LT			CIFAR-100-LT		
Imbalance Factor	200	100	10	200	100	10
End-to-end training						
(1) Softmax	71.2 $\pm$ 0.3	77.4 $\pm$ 0.8	90.0 $\pm$ 0.2	41.0 $\pm$ 0.3	45.3 $\pm$ 0.3	61.9 $\pm$ 0.1
(2) Balanced Softmax $\frac{1}{4}$	71.6 $\pm$ 0.7	78.4 $\pm$ 0.9	90.5 $\pm$ 0.1	41.9 $\pm$ 0.2	46.4 $\pm$ 0.7	62.6 $\pm$ 0.3
(3) Balanced Softmax	<b>79.0 <math>\pm</math> 0.8</b>	<b>83.1 <math>\pm</math> 0.4</b>	<b>90.9 <math>\pm</math> 0.4</b>	<b>45.9 <math>\pm</math> 0.3</b>	<b>50.3 <math>\pm</math> 0.3</b>	<b>63.1 <math>\pm</math> 0.2</b>
Decoupled training						
(4) Balanced Softmax $\frac{1}{4}$ + DT	72.2 $\pm$ 0.1	79.1 $\pm$ 0.2	90.2 $\pm$ 0.0	42.3 $\pm$ 0.0	46.1 $\pm$ 0.1	62.5 $\pm$ 0.1
(5) Balanced Softmax $\frac{1}{4}$ + DT + MS	76.2 $\pm$ 0.4	81.4 $\pm$ 0.1	91.0 $\pm$ 0.1	44.1 $\pm$ 0.2	49.2 $\pm$ 0.1	62.8 $\pm$ 0.2
(6) Balanced Softmax+DT	78.6 $\pm$ 0.1	83.7 $\pm$ 0.1	91.2 $\pm$ 0.0	45.1 $\pm$ 0.0	50.4 $\pm$ 0.0	63.4 $\pm$ 0.0
(7) Balanced Softmax+CBS+DT	80.6 $\pm$ 0.1	84.8 $\pm$ 0.0	91.2 $\pm$ 0.1	42.0 $\pm$ 0.0	47.4 $\pm$ 0.2	62.3 $\pm$ 0.0
(8) DT+MS	73.6 $\pm$ 0.2	79.9 $\pm$ 0.4	90.9 $\pm$ 0.1	44.2 $\pm$ 0.1	49.2 $\pm$ 0.1	63.0 $\pm$ 0.0
(9) Balanced Softmax+DT+MR	79.2 $\pm$ 0.0	84.1 $\pm$ 0.0	91.2 $\pm$ 0.1	45.3 $\pm$ 0.3	50.8 $\pm$ 0.0	63.5 $\pm$ 0.1
(10) BALMS	<b>81.5 <math>\pm</math> 0.0</b>	<b>84.9 <math>\pm</math> 0.1</b>	<b>91.3 <math>\pm</math> 0.1</b>	<b>45.5 <math>\pm</math> 0.1</b>	<b>50.8 <math>\pm</math> 0.0</b>	<b>63.0 <math>\pm</math> 0.1</b>

Table 5: Component Analysis on CIFAR-10/100-LT. DT: decoupled training. CBS: class-balanced sampling. MS: Meta Sampler. MR: Meta Reweighter. Balanced Softmax  $\frac{1}{4}$ : the loss variant in Eqn. 10. Balanced Softmax and Meta Sampler both contribute to the final performance.

**Balanced Softmax.** Comparing (1), (2) with (3), and (5), (8) with (10), we observe that Balanced Softmax gives a clear improvement to the overall performance, under both end-to-end training and decoupled training setup. It successfully accommodates the distribution shift between training and testing. In particular, we observe that Balanced Softmax  $\frac{1}{4}$ , which we derive in Eqn. 10, cannot yield ideal results, compared to our proposed Balanced Softmax in Eqn. 4.

**Meta-Sampler.** From (6), (7), (9) and (10), we observe that Meta-Sampler generally improves the performance, when compared with no Meta-Sampler, and variants of Meta-Sampler. We notice that the performance gain is larger with higher imbalance factor, which is consistent with our observation in LVIS experiments. In (9) and (10), Meta-Sampler generally outperforms the Meta-Reweighter and suggests the discrete sampling process gives a more efficient optimization process. Comparing (7) and (10), we can see Meta-Sampler addresses the over-balancing issue discussed in Section 3.2.

**Decoupled Training.** Comparing (2) with (4) and (3) with (6), decoupled training scheme and Balanced Softmax are two orthogonal components and we can benefit from both at the same time.

## 5 Conclusion

We have introduced BALMS for long-tail visual recognition tasks. BALMS tackles the distribution shift between training and testing, combining meta learning with generalization error bound theory: it optimizes a Balanced Softmax function which theoretically minimizes the generalization error bound; it improves the optimization in large long-tailed datasets by learning an effective Meta Sampler. BALMS generally outperforms SOTA methods on 4 image classification datasets and 1 instance segmentation dataset by a large margin, especially when the imbalance factor is high.



However, Meta Sampler is computationally expensive in practice and the optimization on large datasets is slow. In addition, the Balanced Softmax function only approximately guarantees a generalization error bound. Future work may extend current framework to a wider range of tasks, e.g., machine translation, and correspondingly design tighter bounds and computationally efficient meta-learning algorithms.

## Broader Impact

Due to the Zipfian distribution of categories in real life, algorithms, and models with exceptional performance on research benchmarks may not remain powerful in the real world. BALMS, as a light-weight method, only adds minimal computational cost during training and is compatible with most of the existing works for visual recognition. As a result, BALMS could be beneficial to bridge the gap between research benchmarks and industrial applications for visual recognition.

However, there can be some potential negative effects. As BALMS empowers deep classifiers with stronger recognition capability on long-tailed distribution, the application of such a classification algorithm can be further extended to more real-life scenarios. We should be cautious about the misuse of the method proposed. Depending on the scenario, it might cause negative effect on democratic privacy, e.g., Person ReID, Detection and etc.

## References

- [1] Ricardo Barandela, E Rangel, Jose Salvador Sanchez, and Francesc J Ferri. Restricted decontamination for the imbalanced training sample problem. *Iberoamerican Congress on Pattern Recognition*, 21(9):1263–1284, 2009.
- [2] Mateusz Buda, Atsuto Maki, and Maciej A Mazurowski. A systematic study of the class imbalance problem in convolutional neural networks. *Neural Networks*, 106:249–259, 2018.
- [3] Jonathon Byrd and Zachary C Lipton. What is the effect of importance weighting in deep learning? *arXiv preprint arXiv:1812.03372*, 2018.
- [4] Kaidi Cao, Colin Wei, Adrien Gaidon, Nikos Arechiga, and Tengyu Ma. Learning imbalanced datasets with label-distribution-aware margin loss. In H. Wallach, H. Larochelle, A. Beygelzimer, F. d’Alché-Buc, E. Fox, and R. Garnett, editors, *Advances in Neural Information Processing Systems 32*, pages 1567–1578. Curran Associates, Inc., 2019.
- [5] Nitesh V. Chawla, Kevin W. Bowyer, Lawrence O. Hall, and W. Philip Kegelmeyer. Smote: Synthetic minority over-sampling technique. *Journal of Artificial Intelligence Research*, 16: 321–357, 2002.
- [6] Yin Cui, Menglin Jia, Tsung-Yi Lin, Yang Song, and Serge J. Belongie. Class-balanced loss based on effective number of samples. *2019 IEEE/CVF Conference on Computer Vision and Pattern Recognition (CVPR)*, pages 9260–9269, 2019.
- [7] J. Deng, W. Dong, R. Socher, L.-J. Li, K. Li, and L. Fei-Fei. ImageNet: A Large-Scale Hierarchical Image Database. In *CVPR09*, 2009.
- [8] Edward Grefenstette, Brandon Amos, Denis Yarats, Phu Mon Htut, Artem Molchanov, Franziska Meier, Douwe Kiela, Kyunghyun Cho, and Soumith Chintala. Generalized inner loop meta-learning. *arXiv preprint arXiv:1910.01727*, 2019.
- [9] Agrim Gupta, Piotr Dollar, and Ross Girshick. LVIS: A dataset for large vocabulary instance segmentation. In *Proceedings of the IEEE Conference on Computer Vision and Pattern Recognition*, 2019.
- [10] Hui Han, Wen-Yuan Wang, and Bing-Huan Mao. Borderline-smote: a new over-sampling method in imbalanced data sets learning. *International Conference on Intelligent Computing*, 16:321–357, 2005.

- [11] Munawar Hayat, Salman Khan, Syed Waqas Zamir, Jianbing Shen, and Ling Shao. Gaussian affinity for max-margin class imbalanced learning. In *The IEEE International Conference on Computer Vision (ICCV)*, October 2019.
- [12] H. He and E. A. Garcia. Learning from imbalanced data. *IEEE Transactions on Knowledge and Data Engineering*, 21(9):1263–1284, 2009.
- [13] Chen Huang, Yining Li, Chen Change Loy, and Xiaoou Tang. Learning deep representation for imbalanced classification. In *Proceedings of the IEEE conference on computer vision and pattern recognition*, pages 5375–5384, 2016.
- [14] Chen Huang, Yining Li, Change Loy Chen, and Xiaoou Tang. Deep imbalanced learning for face recognition and attribute prediction. *IEEE transactions on pattern analysis and machine intelligence*, 2019.
- [15] Muhammad Abdullah Jamal, Matthew Brown, Ming-Hsuan Yang, Liqiang Wang, and Boqing Gong. Rethinking class-balanced methods for long-tailed visual recognition from a domain adaptation perspective. *ArXiv*, abs/2003.10780, 2020.
- [16] Eric Jang, Shixiang Gu, and Ben Poole. Categorical reparametrization with gumbel-softmax. In *Proceedings International Conference on Learning Representations 2017*, April 2017.
- [17] Sham M Kakade, Karthik Sridharan, and Ambuj Tewari. On the complexity of linear prediction: Risk bounds, margin bounds, and regularization. In *Advances in neural information processing systems*, pages 793–800, 2009.
- [18] Bingyi Kang, Saining Xie, Marcus Rohrbach, Zhicheng Yan, Albert Gordo, Jiashi Feng, and Yannis Kalantidis. Decoupling representation and classifier for long-tailed recognition. *International Conference on Learning Representations*, abs/1910.09217, 2020.
- [19] Salman Khan, Mohammed Bennamoun, Ferdous Sohel, and Roberto Togneri. Cost-sensitive learning of deep feature representations from imbalanced data. *IEEE Transactions on Neural Networks and Learning Systems*, PP, 08 2015.
- [20] Diederik P Kingma and Jimmy Ba. Adam: A method for stochastic optimization. *International Conference on Learning Representations*, 2015.
- [21] Alex Krizhevsky. Learning multiple layers of features from tiny images. Technical report, 2009.
- [22] Miroslav Kubat and Stan Matwin. Addressing the curse of imbalanced training sets: One-sided selection. In *In Proceedings of the Fourteenth International Conference on Machine Learning*, pages 179–186. Morgan Kaufmann, 1997.
- [23] Buyu Li, Yu Liu, and Xiaogang Wang. Gradient harmonized single-stage detector. In *AAAI Conference on Artificial Intelligence*, 2019.
- [24] Tsung-Yi Lin, Michael Maire, Serge J. Belongie, James Hays, Pietro Perona, Deva Ramanan, Piotr Dollár, and C. Lawrence Zitnick. Microsoft coco: Common objects in context. *ArXiv*, abs/1405.0312, 2014.
- [25] Tsung-Yi Lin, Priya Goyal, Ross B. Girshick, Kaiming He, and Piotr Dollár. Focal loss for dense object detection. *2017 IEEE International Conference on Computer Vision (ICCV)*, pages 2999–3007, 2017.
- [26] Ziwei Liu, Zhongqi Miao, Xiaohang Zhan, Jiayun Wang, Boqing Gong, and Stella X. Yu. Large-scale long-tailed recognition in an open world. *2019 IEEE/CVF Conference on Computer Vision and Pattern Recognition (CVPR)*, pages 2532–2541, 2019.
- [27] I. Loshchilov and F. Hutter. Sgdr: Stochastic gradient descent with warm restarts. In *International Conference on Learning Representations*, April 2017.
- [28] Tomas Mikolov, Ilya Sutskever, Kai Chen, Greg S Corrado, and Jeff Dean. Distributed representations of words and phrases and their compositionality. In C. J. C. Burges, L. Bottou, M. Welling, Z. Ghahramani, and K. Q. Weinberger, editors, *Advances in Neural Information Processing Systems 26*, pages 3111–3119. Curran Associates, Inc., 2013.

- [29] Adam Paszke, Sam Gross, Francisco Massa, Adam Lerer, James Bradbury, Gregory Chanan, Trevor Killeen, Zeming Lin, Natalia Gimelshein, Luca Antiga, Alban Desmaison, Andreas Kopf, Edward Yang, Zachary DeVito, Martin Raison, Alykhan Tejani, Sasank Chilamkurthy, Benoit Steiner, Lu Fang, Junjie Bai, and Soumith Chintala. Pytorch: An imperative style, high-performance deep learning library. In H. Wallach, H. Larochelle, A. Beygelzimer, F. d'Alché-Buc, E. Fox, and R. Garnett, editors, *Advances in Neural Information Processing Systems* 32, pages 8024–8035. 2019.
- [30] Mengye Ren, Wenyuan Zeng, Bin Yang, and Raquel Urtasun. Learning to reweight examples for robust deep learning. In *ICML*, 2018.
- [31] Li Shen, Zhouchen Lin, and Qingming Huang. Relay backpropagation for effective learning of deep convolutional neural networks. In *European conference on computer vision*, pages 467–482. Springer, 2016.
- [32] Jun Shu, Qi Xie, Lixuan Yi, Qian Zhao, Sanping Zhou, Zongben Xu, and Deyu Meng. Meta-weight-net: Learning an explicit mapping for sample weighting. In *Advances in Neural Information Processing Systems*, pages 1917–1928, 2019.
- [33] Hyun Oh Song, Yu Xiang, Stefanie Jegelka, and Silvio Savarese. Deep metric learning via lifted structured feature embedding. In *Computer Vision and Pattern Recognition (CVPR)*, 2016.
- [34] Jingru Tan, Changbao Wang, Buyu Li, Quanquan Li, Wanli Ouyang, Changqing Yin, and Junjie Yan. Equalization loss for long-tailed object recognition. *ArXiv*, abs/2003.05176, 2020.
- [35] Yu-Xiong Wang, Deva Ramanan, and Martial Hebert. Learning to model the tail. In *Advances in Neural Information Processing Systems*, pages 7029–7039, 2017.
- [36] X. Zhang, Z. Fang, Y. Wen, Z. Li, and Y. Qiao. Range loss for deep face recognition with long-tailed training data. In *2017 IEEE International Conference on Computer Vision (ICCV)*, pages 5419–5428, 2017.
- [37] Bolei Zhou, Agata Lapedriza, Aditya Khosla, Aude Oliva, and Antonio Torralba. Places: A 10 million image database for scene recognition. *IEEE Transactions on Pattern Analysis and Machine Intelligence*, 2017.
- [38] Boyan Zhou, Quan Cui, Xiu-Shen Wei, and Zhaomin Chen. Bbn: Bilateral-branch network with cumulative learning for long-tailed visual recognition. *ArXiv*, abs/1912.02413, 2019.

## Appendix A: Proofs and Derivations

### A.1 Proof to Theorem 1

Observe that the conditional probability of a categorical distribution can be parameterized as an exponential family. It gives us a standard Softmax function as an *inverse parameter mapping*

$$\phi_j = \frac{e^{\eta_j}}{\sum_{i=1}^k e^{\eta_i}} \quad (14)$$

and also a *canonical link function*:

$$\eta_j = \log\left(\frac{\phi_j}{\phi_k}\right) \quad (15)$$

We begin by adding a term  $-\log(\phi_j/\hat{\phi}_j)$  to both sides of Eqn. 15,

$$\eta_j - \log \frac{\phi_j}{\hat{\phi}_j} = \log\left(\frac{\phi_j}{\phi_k}\right) - \log\left(\frac{\phi_j}{\hat{\phi}_j}\right) = \log\left(\frac{\hat{\phi}_j}{\phi_k}\right) \quad (16)$$

Subsequently,

$$\phi_k e^{\eta_j - \log \frac{\phi_j}{\hat{\phi}_j}} = \hat{\phi}_j \quad (17)$$

$$\phi_k \sum_{i=1}^k e^{\eta_i - \log \frac{\phi_i}{\hat{\phi}_i}} = \sum_{i=1}^k \hat{\phi}_i = 1 \quad (18)$$

$$\phi_k = 1 / \sum_{i=1}^k e^{\eta_i - \log \frac{\phi_i}{\hat{\phi}_i}} \quad (19)$$

Substitute Eqn. 19 back to Eqn. 17, we have

$$\hat{\phi}_j = \phi_k e^{\eta_j - \log \frac{\phi_j}{\hat{\phi}_j}} = \frac{e^{\eta_j - \log \frac{\phi_j}{\hat{\phi}_j}}}{\sum_{i=1}^k e^{\eta_i - \log \frac{\phi_i}{\hat{\phi}_i}}} \quad (20)$$

Recall that

$$\phi_j = p(y = j|x) = \frac{p(x|y = j)}{p(x)} \frac{1}{k}; \quad \hat{\phi}_j = \hat{p}(y = j|x) = \frac{p(x|y = j)}{\hat{p}(x)} \frac{n_j}{n} \quad (21)$$

then

$$\log \frac{\phi_j}{\hat{\phi}_j} = \log \frac{n}{kn_j} + \log \frac{\hat{p}(x)}{p(x)} \quad (22)$$

Finally, bring Eqn. 22 back to Eqn. 20

$$\hat{\phi}_j = \frac{e^{\eta_j - \log \frac{n}{kn_j} - \log \frac{\hat{p}(x)}{p(x)}}}{\sum_{i=1}^k e^{\eta_i - \log \frac{n}{kn_i} - \log \frac{\hat{p}(x)}{p(x)}}} = \frac{n_j e^{\eta_j}}{\sum_{i=1}^k n_i e^{\eta_i}} \quad (23)$$

### A.2 Derivation for the Multiple Binary Logistic Regression variant

**Definition.** Multiple Binary Logistic Regression uses  $k$  binary logistic regression to do multi-class classification. Same as Softmax regression, the predicted label is the class with the maximum model output,

$$y_{pred} = \arg \max_j (\eta_j). \quad (24)$$

The only difference is that  $\phi_j$  is expressed by a logistic function of  $\eta_j$

$$\phi_j = \frac{e^{\eta_j}}{1 + e^{\eta_j}} \quad (25)$$

and the loss function sums up binary classification loss on all classes

$$l(\theta) = \sum_{j=1}^k -\log \tilde{\phi}_j \quad (26)$$

where

$$\tilde{\phi}_j = \begin{cases} \phi_j, & \text{if } y = j \\ 1 - \phi_j, & \text{otherwise} \end{cases} \quad (27)$$

**Setup.** By the virtue of Bayes Rule,  $\phi_j$  and  $1 - \phi_j$  can be decomposed as

$$\phi_j = \frac{p(x|y=j)p(y=j)}{p(x)}; \quad 1 - \phi_j = \frac{p(x|y \neq j)p(y \neq j)}{p(x)} \quad (28)$$

and for  $\hat{\phi}$  and  $1 - \hat{\phi}$ ,

$$\hat{\phi}_j = \frac{p(x|y=j)\hat{p}(y=j)}{\hat{p}(x)}; \quad 1 - \hat{\phi}_j = \frac{p(x|y \neq j)\hat{p}(y \neq j)}{\hat{p}(x)} \quad (29)$$

**Derivation.** Again, we introduce the exponential family parameterization and have the following link function for  $\phi_j$

$$\eta_j = \log \frac{\phi_j}{1 - \phi_j} \quad (30)$$

Bring the decomposition Eqn. 28 and Eqn.29 into the link function above

$$\eta_j = \log\left(\frac{\hat{\phi}_j}{1 - \hat{\phi}_j} \cdot \frac{\phi_j}{\hat{\phi}_j} \cdot \frac{1 - \hat{\phi}_j}{1 - \phi_j}\right) \quad (31)$$

$$\eta_j = \log\left(\frac{\hat{\phi}_j}{1 - \hat{\phi}_j} \cdot \frac{p(x|y=j)p(y=j)/p(x)}{p(x|y=j)\hat{p}(y=j)/\hat{p}(x)} \cdot \frac{p(x|y \neq j)\hat{p}(y \neq j)/\hat{p}(x)}{p(x|y \neq j)p(y \neq j)/p(x)}\right) \quad (32)$$

Simplify the above equation

$$\eta_j = \log\left(\frac{\hat{\phi}_j}{1 - \hat{\phi}_j} \cdot \frac{p(y=j)}{\hat{p}(y=j)} \cdot \frac{\hat{p}(y \neq j)}{p(y \neq j)}\right) \quad (33)$$

Substitute the  $n_j$  in to the equation above

$$\eta_j = \log\left(\frac{\hat{\phi}_j}{1 - \hat{\phi}_j} \cdot \frac{n/k}{n_j} \cdot \frac{n - n_j}{n - n/k}\right) \quad (34)$$

Then

$$\eta_j - \log\left(\frac{n/k}{n_j} \cdot \frac{n - n_j}{n - n/k}\right) = \log\left(\frac{\hat{\phi}_j}{1 - \hat{\phi}_j}\right) \quad (35)$$

Finally, we have

$$\hat{\phi}_j = \frac{e^{\eta_j - \log(\frac{n/k}{n_j} \cdot \frac{n - n_j}{n - n/k})}}{1 + e^{\eta_j - \log(\frac{n/k}{n_j} \cdot \frac{n - n_j}{n - n/k})}} \quad (36)$$

### A.3 Proof to Theorem 2

**Setup.** Firstly, we define  $f$  as,

$$f(x) := -l(\theta) + t \quad (37)$$

where  $l(\theta)$  and  $t$  is previously defined in submission. However,  $f$  does not have a specific semantic meaning as it is defined only to keep consistent with notations in [17].

Let  $err_j(t)$  be the 0-1 loss on example from class  $j$

$$err_j(t) = \Pr_{(x,y) \in S_j} [f(x) < 0] = \Pr_{(x,y) \in S_j} [l(\theta) > t] \quad (38)$$

and  $err_{\gamma,j}(t)$  be the 0-1 margin loss on example from class  $j$

$$err_{\gamma,j}(t) = \Pr_{(x,y) \in S_j} [f(x) < \gamma_j] = \Pr_{(x,y) \in S_j} [l(\theta) + \gamma_j > t] \quad (39)$$

Let  $\hat{err}_{\gamma,j}(t)$  denote the empirical variant of  $err_{\gamma,j}(t)$ .

**Proof.** For any  $\delta > 0$  and with probability at least  $1 - \delta$ , for all  $\gamma_j > 0$ , and  $f \in \mathcal{F}$ , Theorem 2 in [17] directly gives us

$$err_j(t) \leq \hat{err}_{\gamma,j}(t) + \frac{4}{\gamma_j} \hat{\mathfrak{R}}_j(\mathcal{F}) + \sqrt{\frac{\log(\log_2 \frac{4B}{\gamma_j})}{n_j}} + \sqrt{\frac{\log(1/\delta)}{2n_j}} \quad (40)$$

where  $\sup_{(x,y) \in S} |l(\theta) - t| \leq B$  and  $\hat{\mathfrak{R}}_j(\mathcal{F})$  denotes the empirical Rademacher complexity of function family  $\mathcal{F}$ . By applying [4]'s analysis on the empirical Rademacher complexity and union bound over all classes, we have the generalization error bound for the loss on a balanced test set

$$err_{bal}(t) \leq \frac{1}{k} \sum_{j=1}^k \left( \hat{err}_{\gamma,j}(t) + \frac{4}{\gamma_j} \sqrt{\frac{C(\mathcal{F})}{n_j}} + \epsilon_j(\gamma_j) \right) \quad (41)$$

where

$$\epsilon_j(\gamma_j) \triangleq \sqrt{\frac{\log(\log_2 \frac{4B}{\gamma_j})}{n_j}} + \sqrt{\frac{\log(1/\delta)}{2n_j}} \quad (42)$$

is a low-order term of  $n_j$ . To minimize the generalization error bound Eqn. 41, we essentially need to minimize

$$\sum_{j=1}^k \frac{4}{\gamma_j} \sqrt{\frac{C(\mathcal{F})}{n_j}} \quad (43)$$

By constraining the sum of  $\gamma$  as  $\sum_{j=1}^k \gamma_j = \beta$ , we can directly apply Cauchy-Schwarz inequality to solve the optimal  $\gamma$

$$\gamma_j^* = \frac{\beta n_j^{-1/4}}{\sum_{i=1}^k n_i^{-1/4}}. \quad (44)$$

#### A.4 Proof to Corollary 2.1

**Preliminary.** Notice that  $\hat{l}_j^*(\theta) = l_j(\theta) + \gamma_j^*$  can not be achieved, because  $-\log \hat{\phi}_j^* = -\log \phi_j + \gamma_j^*$  and  $\gamma_j^* > 0$  implies

$$\hat{\phi}_j^* < \phi_j; \quad \sum_{j=1}^k \hat{\phi}_j^* < \sum_{j=1}^k \phi_j = 1 \quad (45)$$

The equation above contradicts with the definition that sum of  $\hat{\phi}^*$  should be exactly equal to 1. To solve the contradiction, we introduce a term  $\gamma_{base} > 0$ , such that

$$-\log \hat{\phi}_j^* = -\log \phi_j - \gamma_{base} + \gamma_j^*; \quad \sum_{j=1}^k \hat{\phi}_j^* = 1 \quad (46)$$

To justify the new term  $\gamma_{base}$ , we recall the definition of error

$$err_{\gamma,j}(t) = \Pr_{(x,y) \in S_j} [l(\theta) + \gamma_j > t]; \quad err_{bal}(t) = \Pr_{(x,y) \in S_{bal}} [l(\theta) > t] \quad (47)$$

If we tweak the threshold  $t$  with the term  $\gamma_{base}$

$$err_{\gamma,j}(t + \gamma_{base}) = \Pr_{(x,y) \in S_j} [l(\theta) + \gamma_j > t + \gamma_{base}] = \Pr_{(x,y) \in S_j} [(l(\theta) - \gamma_{base}) + \gamma_j > t] \quad (48)$$

$$err_{bal}(t + \gamma_{base}) = \Pr_{(x,y) \in S_{bal}} [l(\theta) > t + \gamma_{base}] = \Pr_{(x,y) \in S_{bal}} [(l(\theta) - \gamma_{base}) > t] \quad (49)$$

As  $\gamma^*$  is not a function of  $t$ , the value of  $\gamma^*$  will not be affected by the tweak. Thus, instead of looking for  $\hat{l}_j^*(\theta) = l_j(\theta) + \gamma_j^*$  that minimizes the generalization bound for  $err_{bal}(t)$ , we are in fact looking for  $\hat{l}_j^*(\theta) = (l_j(\theta) - \gamma_{base}) + \gamma_j^*$  that minimizes generalization bound for  $err_{bal}(t + \gamma_{base})$

**Proof.** In this section, we show that  $\hat{l}_j$  in the corollary is an approximation of  $\hat{l}_j^*$ .

$$\hat{l}_j(\theta) - (l_j(\theta) - \gamma_{base}) = \log \phi_j - \log \hat{\phi}_j + \gamma_{base} \quad (50)$$

$$= \log \frac{e^{\eta_j}}{\sum_{i=1}^k e^{\eta_i}} - \log \frac{e^{\eta_j - \log \gamma_j^*}}{\sum_{i=1}^k e^{\eta_i - \log \gamma_i^*}} + \gamma_{base} \quad (51)$$

$$= \log \frac{e^{\eta_j}}{\sum_{i=1}^k e^{\eta_i}} - \log \frac{e^{\eta_j}}{\sum_{i=1}^k e^{\eta_i - \log \gamma_i^* + \log \gamma_j^*}} + \gamma_{base} \quad (52)$$

$$= \log \sum_{i=1}^k e^{\eta_i - \log \gamma_i^* + \log \gamma_j^*} - \log \sum_{i=1}^k e^{\eta_i} + \gamma_{base} \quad (53)$$

$$= \left( \sum_{i=1}^k e^{\eta_i - \log \gamma_i^* + \log \gamma_j^*} - \sum_{i=1}^k e^{\eta_i} \right) / \alpha + \gamma_{base} \quad (\text{Mean-Value Theorem}) \quad (54)$$

$$= (\gamma_j^* \sum_{i=1}^k \frac{1}{\gamma_i^*} e^{\eta_i} - \sum_{i=1}^k e^{\eta_i}) / \alpha + \gamma_{base} \quad (55)$$

$$\geq \left( \frac{\gamma_j^*}{\beta} \left( \sum_{i=1}^k e^{\frac{1}{2} \eta_i} \right)^2 - \sum_{i=1}^k e^{\eta_i} \right) / \alpha + \gamma_{base} \quad (\text{Cauchy-Schwarz Inequality}) \quad (56)$$

$$= (\gamma_j^* \frac{\lambda}{\beta} \sum_{i=1}^k e^{\eta_i} - \sum_{i=1}^k e^{\eta_i}) / \alpha + \gamma_{base} \quad (1 \leq \lambda \leq k) \quad (57)$$

$$\approx \gamma_j^* \quad (\text{given } \beta = \lambda, \gamma_{base} = 1) \quad (58)$$

$$(59)$$

where  $\alpha = \frac{d}{dx} \log(x')$  for some  $x'$  in between  $\sum_{i=1}^k e^{\eta_i - \log \gamma_i^* + \log \gamma_j^*}$  and  $\sum_{i=1}^k e^{\eta_i}$ ,  $\lambda$  is close to a constant when the model converges. Although the approximation holds under some constraints, we show that it approximately minimizes the generalization bound derived in the last section.

## A.5 Derivation for Eqn.12

Gradient for positive samples:

$$\frac{\partial \hat{l}_{y=j}^{(s)}(\theta)}{\partial \theta_j} = \frac{\partial - \log \hat{\phi}_j^{(s)}}{\partial \theta_j} \quad (60)$$

$$= \frac{\partial - \log \frac{e^{\theta_j^T f(x^{(s)}) + \log n_j}}{\sum_{i=1}^n e^{\theta_i^T f(x^{(s)}) + \log n_i}}}{\partial \theta_j} \quad (61)$$

$$= - \frac{\partial \theta_j^T f(x^{(s)}) + \log n_j}{\partial \theta_j} + \frac{\partial \log \sum_{i=1}^n e^{\theta_i^T f(x^{(s)}) + \log n_i}}{\partial \theta_j} \quad (62)$$

$$= -f(x^{(s)}) + f(x^{(s)}) \frac{e^{\theta_j^T f(x^{(s)}) + \log n_j}}{\sum_{i=1}^n e^{\theta_i^T f(x^{(s)}) + \log n_i}} \quad (63)$$

$$= -f(x^{(s)}) + f(x^{(s)}) \hat{\phi}_j^{(s)} \quad (64)$$

$$= f(x^{(s)}) (\hat{\phi}_j^{(s)} - 1) \quad (65)$$

Gradient for negative samples:

$$\frac{\partial \hat{l}_{y \neq j}^{(s)}(\theta)}{\partial \theta_j} = \frac{\partial -\log \hat{\phi}_y^{(s)}}{\partial \theta_j} \quad (66)$$

$$= \frac{\partial -\log \frac{e^{\theta_y^T f(x^{(s)}) + \log n_y}}{\sum_{i=1}^n e^{\theta_i^T f(x^{(s)}) + \log n_i}}}{\partial \theta_j} \quad (67)$$

$$= -\frac{\partial \theta_y^T f(x^{(s)}) + \log n_y}{\partial \theta_j} + \frac{\partial \log \sum_{i=1}^n e^{\theta_i^T f(x^{(s)}) + \log n_i}}{\partial \theta_j} \quad (68)$$

$$= f(x^{(s)}) \frac{e^{\theta_j^T f(x^{(s)}) + \log n_j}}{\sum_{i=1}^n e^{\theta_i^T f(x^{(s)}) + \log n_i}} \quad (69)$$

$$= f(x^{(s)}) \hat{\phi}_j^{(s)} \quad (70)$$

Overall gradients on the training dataset:

$$\sum_{s=1}^n l^{(s)}(\theta) = \sum_{s=1}^{n_j} l_{y=j}^{(s)}(\theta) + \sum_{i \neq j}^k \sum_{s=1}^{n_i} l_{y=i}^{(s)}(\theta) \quad (71)$$

$$= \sum_{s=1}^{n_j} f(x^{(s)}) (\hat{\phi}_j^{(s)} - 1) + \sum_{i \neq j}^k \sum_{s=1}^{n_i} f(x^{(s)}) \hat{\phi}_j^{(s)} \quad (72)$$

With Class-Balanced Sampling (CBS), number of samples in each class is equalized and therefore changed from  $n_i$  and  $n_j$  to  $B/k$

$$\sum_{s=1}^B l^{(s)}(\theta) = \sum_{s=1}^{B/k} f(x^{(s)}) (\hat{\phi}_j^{(s)} - 1) + \sum_{i \neq j}^k \sum_{s=1}^{B/k} f(x^{(s)}) \hat{\phi}_j^{(s)} \quad (73)$$

Set the overall gradient of a training batch to be zero gives

$$\sum_{s=1}^{B/k} f(x^{(s)}) (1 - \hat{\phi}_j^{(s)}) - \sum_{i \neq j}^k \sum_{s=1}^{B/k} f(x^{(s)}) \hat{\phi}_j^{(s)} = 0 \quad (74)$$

We can also rewrite the equation using empirical expectation

$$\frac{1}{n_j} \mathbb{E}_{(x^+, y=j) \sim D_{train}} [f(x^+) (1 - \hat{\phi}_j)] - \sum_{i \neq j}^k \frac{1}{n_i} \mathbb{E}_{(x^-, y=i) \sim D_{train}} [f(x^-) \hat{\phi}_j] = 0 \quad (75)$$

Then we make the following approximation when the training loss is close to 0, i.e.,  $\hat{\phi}_y \rightarrow 1$

$$\lim_{\hat{\phi}_y \rightarrow 1} \frac{n_y e^{\eta_y}}{n_y e^{\eta_y} + \sum_{i \neq y}^k n_i e^{\eta_i}} = 1 \quad (76)$$

$$\lim_{\hat{\phi}_y \rightarrow 1} \frac{1}{1 + \sum_{i \neq y}^k \frac{n_i}{n_y} e^{\eta_i - \eta_y}} = 1 \quad (77)$$

$$\lim_{\hat{\phi}_y \rightarrow 1} \sum_{i \neq y}^k e^{\eta_i - \eta_y} = 0 \quad (78)$$



for positive samples:

$$\lim_{\hat{\phi}_y=j \rightarrow 1} \hat{\phi}_j / \phi_j = \lim_{\hat{\phi}_y=j \rightarrow 1} \frac{n_j e^{\eta_j}}{n_j e^{\eta_j} + \sum_{i \neq y}^k e^{\eta_i}} / \frac{e^{\eta_j}}{e^{\eta_j} + \sum_{i \neq y}^k e^{\eta_i}} \quad (79)$$

$$= \lim_{\hat{\phi}_y=j \rightarrow 1} \frac{n_j e^{\eta_j}}{e^{\eta_j}} \cdot \frac{e^{\eta_j} + \sum_{i \neq y}^k e^{\eta_i}}{n_j e^{\eta_j} + \sum_{i \neq y}^k e^{\eta_i}} \quad (80)$$

$$= \lim_{\hat{\phi}_y=j \rightarrow 1} n_j \cdot \frac{1 + \sum_{i \neq y}^k e^{\eta_i - \eta_j}}{n_j + \sum_{i \neq y}^k e^{\eta_i - \eta_j}} \quad (81)$$

$$= \lim_{\hat{\phi}_y=j \rightarrow 1} n_j \cdot \frac{1 + 0}{n_j + 0} \quad (82)$$

$$= 1 \quad (83)$$

for negative samples:

$$\lim_{\hat{\phi}_y \neq j \rightarrow 1} \hat{\phi}_j / \phi_j = \lim_{\hat{\phi}_y \neq j \rightarrow 1} \frac{n_j e^{\eta_j}}{n_y e^{\eta_y} + \sum_{i \neq y}^k e^{\eta_i}} / \frac{e^{\eta_j}}{e^{\eta_j} + \sum_{i \neq y}^k e^{\eta_i}} \quad (84)$$

$$= \lim_{\hat{\phi}_y \neq j \rightarrow 1} \frac{n_j e^{\eta_j}}{e^{\eta_j}} \cdot \frac{e^{\eta_j} + \sum_{i \neq y}^k e^{\eta_i}}{n_y e^{\eta_y} + \sum_{i \neq y}^k e^{\eta_i}} \quad (85)$$

$$= \lim_{\hat{\phi}_y \neq j \rightarrow 1} n_j \cdot \frac{1 + \sum_{i \neq y}^k e^{\eta_i - \eta_j}}{n_y + \sum_{i \neq y}^k e^{\eta_i - \eta_j}} \quad (86)$$

$$= \lim_{\hat{\phi}_y \neq j \rightarrow 1} n_j \cdot \frac{1 + 0}{n_y + 0} \quad (87)$$

$$= n_j / n_y \quad (88)$$

Therefore, when  $\hat{\phi}_y \rightarrow 1$ , Eqn.75 can be expanded as

$$\frac{1}{n_j} \mathbb{E}_{(x^+, y=j) \sim D_{train}} [f(x^+) (1 - \phi_j)] - \sum_{i \neq j}^k \frac{1}{n_i} \mathbb{E}_{(x^-, y=i) \sim D_{train}} [f(x^-) \phi_j \frac{n_j}{n_i}] \approx 0 \quad (89)$$

That is

$$\frac{1}{n_j^2} \mathbb{E}_{(x^+, y=j) \sim D_{train}} [f(x^+) (1 - \phi_j)] - \sum_{i \neq j}^k \frac{1}{n_i^2} \mathbb{E}_{(x^-, y=i) \sim D_{train}} [f(x^-) \phi_j] \approx 0 \quad (90)$$

## Appendix B: Detailed Description for Meta Sampler

### B.1 Meta Sampler

To estimate the optimal sample rate, we first make the sampler differentiable. Normally, class-balanced samplers take following steps:

1. Define a class sample distribution  $\pi = \pi_1^{\mathbf{1}_{\{y=1\}}} \pi_2^{\mathbf{1}_{\{y=2\}}} \dots \pi_k^{\mathbf{1}_{\{y=k\}}}$ .
2. Assign  $\pi_j$  to all instance-label pairs  $(x, y = j)$  and normalize over the dataset, to give the instance sample distribution  $\rho = \rho_1^{\mathbf{1}_{\{i=1\}}} \rho_2^{\mathbf{1}_{\{i=2\}}} \dots \rho_n^{\mathbf{1}_{\{i=n\}}}$ .
3. Draw discrete image indexes from  $\rho$  to form a batch with size  $b$ .
4. Augment the images and feed images into a model.

The steps where discrete sampling and image augmentation happen are usually not differentiable. We propose a simple yet effective method to back-propagate the gradient directly from the loss to the learnable sample rates.

Firstly, we use the Straight-through Gumbel Estimator [16] to approximate the gradient through the multinomial sampling:

$$s_j = \frac{((\log \rho_j + g_j)/\tau)}{\sum_{i=1}^n \exp((\log(\rho_i + g_i)/\tau))} \quad (91)$$

where  $s$  is the sample result,  $g$  is i.i.d. samples drawn from  $\text{Gumbel}(0, 1)$  and  $\tau$  is the temperature coefficient. Straight-through means that we use  $\text{argmax}$  to discretize  $s$  to  $(0,1)$  during forward and use  $\nabla s$  during backward. Gumbel-Softmax re-parameterization is commonly found to have less variance in gradient estimation than score functions [16].

Then, we use an external memory to connect sampler with loss. We use the Straight-through Gumbel Estimator to draw  $b$  discrete samples from  $\rho$ , we denote as  $s^{b \times n}$ .  $s^{b \times n}$  is matrix of a  $n$ -dimensional one-hot vectors, representing  $b$  selected images. Concretely, for the  $i$ -th sample, if the Gumbel Estimator gives a sampling result to be  $c$ -th image, we have  $s^{(i)}$  to be

$$s_j^{(i)} = \begin{cases} 1, & \text{if } j = c \\ 0, & \text{otherwise} \end{cases} \quad (92)$$

We save this matrix into an external memory during data preparation. After obtaining the classification loss  $l(\theta)$ , which is the  $i$ -th loss in the batch computed from the  $c$ -th sample, we re-weight the loss by

$$\tilde{l}^{(i)}(\theta) = l^{(i)}(\theta) \cdot s_c^{(i)} \quad (93)$$

Notice that the re-weight will not change the loss value, it only connects sampling results with the classification loss in the computation graph. By doing so, the gradient from the loss can directly reach the learnable sample rate  $\pi$ .

## B.2 Meta Reweighter

Since one image might contain multiple instances from several categories, we use Meta Reweighter, rather than Meta Sampler on LVIS dataset. Specifically, we assign the loss weight for instance  $i$  to be  $\rho_i = \pi_j$ , where  $\pi$  is a learnable class weight and  $j$  is the class label of instance  $i$ . Next, we perform similar bi-level optimization as in Meta Sampler, where we re-weight the loss of an instance by its loss weight  $\rho_i$  instead of a discrete 0-1 sampling result  $s_i$ .

## Appendix C: Implementation Details

### C.1 Hardware

We use Intel Xeon Gold 6148 CPU @ 2.40GHz with Nvidia V100 GPU for model training. We take single GPU to train models on CIFAR-10-LT, CIFAR-100-LT, ImageNet-LT and Places-LT and 8 GPUs to train models on LVIS.

### C.2 Software

We implement our proposed algorithm with PyTorch-1.3.0 [29] for all experiments. Second-order derivatives are computed with Higher [8] library.

### C.3 Training Details

**Decoupled Training** Through the paper, we refer decoupled training as training on a fixed feature extractor obtained from instance-balanced training, which is consistent with [18].

**CIFAR-10-LT and CIFAR-100-LT** All experiments use ResNet-32 as backbone like [6]. We use Nesterov SGD with momentum 0.9 and weight-decay 0.0005 for training. We use a total mini-batch size of 512 images on a single GPU. The learning rate increased from 0.05 to 0.1 in the first 800 iterations. Cosine scheduler [27] is applied afterward, with minimum learning rate 0. Our augmentation follows [34]. In testing, the image size is 32x32. In end-to-end training, the model is trained for 13K iterations. In decoupled training experiments, we fix the Softmax model, i.e., the instance-balanced baseline model obtained from the previous end-to-end training, as the feature extractor. And the classifier is trained for 2K iterations. For Meta Sampler and Meta Reweighter,

we use Adam[20] with betas (0.9, 0.99) and weight decay 0. The learning rate is set to 0.01 with no warm-up strategy or scheduler applied. The meta-set is formed by randomly sampling 512 images from the training set with replacement, using Class-Balanced Sampling.

**ImageNet-LT and Places-LT** We follow the same setup as [18] for decoupled classifier retraining.

We first train a base model without any bells and whistles following Kang et al. [18] for these two datasets. For ImageNet-LT, the model is trained for 90 epochs from scratch. For Places-LT, we choose ResNet-152 as the backbone network pre-trained on the full ImageNet-2012 dataset and train it on Places-LT following Kang et al [18]. For both datasets, we use SGD optimizer with momentum 0.9, batch size 512, cosine learning rate schedule [27] decaying from 0.2 to 0 and image resolution  $224 \times 224$ .

After obtaining the base model, we retrain the final fully connected layer, i.e., classifier. For Meta Sampler, we use Adam[20] with betas (0.9, 0.99) and weight decay 0. The learning rate is set to 0.01 with no warm-up strategy and is kept unchanged during the training process. The meta-set is formed by randomly sampling 512 images from the training set with replacement, using Class-Balanced Sampling. For ImageNet-LT, we use SGD optimizer with momentum 0.9, batch size 512, cosine learning rate schedule decaying from 0.2 to 0 for 10 epochs. For Places-LT, we use SGD optimizer with momentum 0.9, batch size 128, cosine learning rate schedule decaying from 0.01 to 0 for 10 epochs.

For the training process, we resize the image to  $224 \times 224$ . During testing, we first resize the image to  $256 \times 256$  and do center-crop to obtain an image of  $224 \times 224$ .

**LVIS** We use the off-the-shelf model Mask R-CNN with the backbone network ResNet-50 for LVIS. The backbone network is pre-trained on ImageNet. We follow the setup from the original dataset paper [9] for two baseline models (Softmax and Sigmoid). We use an SGD optimizer with 0.9 momentum, 0.01 initial learning rate, and 0.0001 weight decay. The model is trained for 90k iterations with 8 images per mini-batch. The learning rate is dropped by a factor of 10 at both 60k iterations and 80k iterations.

Methods other than baselines are trained under the retrain scheme [18]. We take the above-mentioned models as the base model and retrained the bounding box classifier with various methods. The bounding box classifier consists of one fully connected layer. We use an SGD optimizer with 0.9 momentum, 0.02 initial learning rate, and 0.0001 weight decay. The model is trained for 22k iterations with 8 images per mini-batch. The learning rate is dropped by a factor of 10 at both 11k iterations and 18k iterations.

For our method with a Meta Reweighter, we use Adam optimizer with 0.001 for the Meta Reweighter and train the Meta Reweighter together with the model. The learning rate is kept unchanged during the training process.

We apply scale jitter and random flip at training time (sampling image scale for the shorter side from 640, 672, 704, 736, 768, 800). For testing, images are resized to a shorter image edge of 800 pixels; no test-time augmentation is used.

#### C.4 Comparison of Balanced Softmax and standard Softmax when Meta Sampler applied

Figure 2 demonstrates that compared with standard Softmax function, Meta Sampler learns a more *balanced* sampling rates with our proposed Balanced Softmax. The sampling rates for all the classes are initialized with 0.5 and are constrained in the range of (0,1).

The blue bar represents the learned sampling rates with standard Softmax. The sampling rates of tail classes approach 1 while the sampling rates of head classes approach 0. Such an extreme divergence in sample rates could potentially lead to overfitting tail classes and underfitting head classes: the same problem as in Class-Balance Sampling (CBS), especially when the imbalance ratio is high. Moreover, the diverged sample rates pose challenges to the meta-learning optimization process. A very low optimal learning rate may also not be numerically stable.

With Balanced Softmax, we can see that Meta Sampler produces a more balanced distribution of sampling rates. After convergence, the sample rates for Softmax has a variance of 0.13. Balanced Softmax significantly reduces the variance to 0.03.

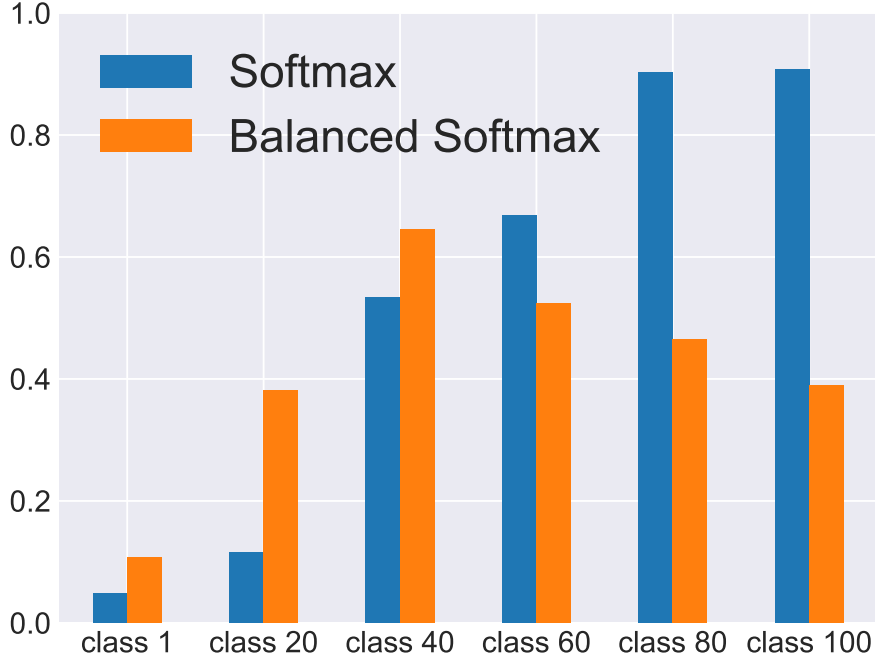


Figure 2: Learned sample rates with Meta-Sampler. The X-axis denotes classes with a decreasing number of training samples. Y-axis denotes sample rates for different classes. Balanced Softmax gives a smoother distribution compared to Softmax.

## Appendix D: More Details Regarding Datasets

### D.1 Basic Information

We hereby provide more details about datasets mentioned in the paper in Table 6

Dataset	#Classes	Imbalance Factor	#Train Instances	Head Class Size	Tail Class Size
CIFAR-10-LT [21]	10	10-200	50,000 – 11,203	5,000	500-25
CIFAR-100-LT [21]	100	10-200	50,000 – 9,502	500	50-2
ImageNet-LT [26]	1,000	256	115,846	1280	5
Places-LT [37]	365	996	62,500	4,980	5
LVIS [9]	1,230	26,148	693,958	26,148	1

Table 6: Details of long-tailed datasets. Notice that for both CIFAR-10-LT and CIFAR-100-LT, the number of tail class varies with different imbalance factors.

All the datasets are publicly available for downloading, we provide the download link as follows: ImageNet, CIFAR-10 and CIFAR-100, Places365, and LVIS.

### D.2 Long-tailed Datasets Generation

**CIFAR10-LT and CIFAR100-LT:** We generated the long-tailed version of CIFAR-10 and CIFAR-100 following Cui et al. [6]. For both the original CIFAR-10 and CIFAR-100, they contain 50000 training images and 10000 test images at a size of  $32 \times 32$  uniformly distributed in 10 classes and 100 classes. The long-tailed version is created by randomly reducing training samples. In particular, the number of samples in the  $y$ -th class is  $n_y \mu^y$ , where  $n_y$  is the original number of training samples

in the class and  $\mu \in (0, 1)$ . By varying  $\mu$ , we generate three training sets with the imbalance factors of 200, 100, and 10. The test set is kept unchanged and balance.

**ImageNet-LT:** We use the long-tailed version of ImageNet from Liu et al. [26]. It is created by firstly sampling the class sizes from a Pareto distribution with the power value  $\alpha = 6$ , followed by sampling the corresponding number of images for each class. The ImageNet-LT dataset has 115,846 training images in 1,000 classes, and its imbalance factor is 256 as shown in Table 6. The original ImageNet [7] validation set is used as the test set, which contains 50 images for each class.

**Places-LT:** In a similar spirit to the long-tailed ImageNet, a long-tailed version of Places-365 dataset is generated using the same strategy as above. It contains 62,500 training images from 365 classes with an imbalance factor 996. In the test set, there are 100 test images for each class.

**LVIS:** We use official training and validation split from LVIS [9]. No modification is made.